Proc. Natl. Acad. Sci. USA
Vol. 90, pp. 5057–5061, June 1993
Biophysics

Molecular cloning, functional expression, and pharmacological characterization of an *N*-methyl-D-aspartate receptor subunit from human brain

(synaptic transmission/ion channels/excitotoxicity/glutamate receptor/neurodegeneration)

ROSA PLANELLS-CASES, WILLIAM SUN, ANTONIO V. FERRER-MONTIEL, AND MAURICIO MONTAL*

Department of Biology, University of California, San Diego, La Jolla, CA 92093-0319

Communicated by Roger Dashen, February 18, 1993 (received for review November 19, 1992)

ABSTRACT **A cDNA encoding a full-length *N*-methyl-D-aspartate (NMDA) receptor subunit 1, hNR1, was isolated from a human brain cDNA library. The hNR1 cDNA encodes an open reading frame of ≈2.7 kb that shares high homology with the rat brain NMDA receptor subunit 1 and the mouse ζ1 subunit. The hNR1 sequence, however, diverges from the rodent and murine homologs near the C terminus, suggesting that they represent alternatively spliced messages of the same gene. Oocytes injected with cRNA synthesized from the hNR1 cDNA express glutamate and NMDA-activated currents in the presence of glycine. Currents are blocked by the NMDA-receptor-specific antagonists 2-amino-5-phosphovaleric acid and 7-chlorokynurenate, and the open channel blockers MK-801 and phencyclidine, by Mg^{2+} ions in a voltage-dependent manner, and by Zn^{2+}. Expressed hNR1 homomeric receptor channels exhibit the high Ca^{2+} permeability characteristic of neuronal NMDA receptors. Therefore, the cDNA clone hNR1 codes for a human brain NMDA receptor subunit cognate to the rodent and murine brain NR1 subunits.**

Glutamate receptors are the subject of intense investigation due to their potential central role in the function (1) and dysfunction (2) of the human brain. These excitatory amino acid receptors have been extensively characterized and classified according to pharmacology (3). One class of these receptors, activated by *N*-methyl-D-aspartate (NMDA), the NMDA receptor, has received special attention based on its involvement in inducing long-term potentiation in the postsynaptic neuron, a phenomenon postulated to underlie some types of learning (4). In addition, the high permeability of this ligand-gated channel to calcium ions increases the susceptibility of neurons to glutamate agonist-induced neurotoxicity resultant from overstimulation. Accordingly, the NMDA receptor may be implicated in mediating excitation-induced neuronal cell death associated with disorders such as stroke, epilepsy, Parkinson disease, and Alzheimer disease (2, 5).

The electrophysiological and pharmacological properties of NMDA receptors have been characterized by patch-clamp recordings from cultured neurons (4, 6, 7). Recently, a cDNA encoding one of its subunits was isolated from rat brain (8). This subunit, NMDAR1 or the murine homolog ζ1 (9), when expressed in *Xenopus laevis* oocytes, forms NMDA receptor channels that exhibit the electrophysiological and pharmacological properties characteristic of the NMDA receptor, including agonist/antagonist specificity, glycine requirement, high Ca^{2+} permeability, and voltage-dependent channel blockade by extracellular Mg^{2+}. Since the cloning of the NMDAR1 subunit, several other subunits of the NMDA receptor have been isolated, including the rodent NR2A, -B, and -C (10) and murine ε1, -2, and -3 subunits (11). The NR2 subunits form functional NMDA receptor channels in amphibian oocytes only when coexpressed with the NR1 subunit, but heteromeric receptors display different electrophysiological properties (10–12). Splice variants of the NMDAR1 subunit or ζ1 subunit cDNA have been identified (9, 13–16), indicating that the *NMDAR* gene undergoes extensive alternative splicing that, in turn, may contribute to the functional diversity of the receptor (1).

The pivotal involvement of and interplay between glutamate receptors, NMDA receptors, and calcium channels in the biology and pathology of central neurons (2, 17) prompted us to clone and characterize the genes coding for members of these receptor and channel superfamilies from human brain (18, 19). Here, we report the isolation of a full-length cDNA clone encoding a human brain NMDA receptor subunit cognate to the rodent NMDA receptor subunit 1 (8, 14, 15) and murine ζ1 subunit (9) and the characterization of the gene product after its expression in *Xenopus* oocytes.†

MATERIALS AND METHODS

Screening the Human Cortex cDNA Library. A cDNA library derived from size-selected human frontal cortex mRNA 2–4 kb in length (18, 19) was screened using a *Bst*XI fragment from the rat NMDA receptor subunit 1 (rNR1) (8) encompassing nt 220–2345 of the coding region. The probe was labeled with digoxigenin-conjugated dUTP (Genius System, Boehringer Mannheim; ref. 20), hybridized to filters (Hybond, Amersham) at 65°C overnight, and detected by binding of alkaline phosphatase-conjugated antibody specific for the digoxigenin hapten (20). Bluescript SK(-) phagemids (Stratagene) were rescued from seven purified positive plaques by an *in vivo* excision protocol. A 1.4-kb *Apa* I fragment from an isolated human partial NMDA receptor cDNA, NM5 (nt −100 to 1316), was ^{32}P-labeled and used to screen the human cortex library containing inserts >4 kb (18, 19). Secondary and purification screenings were done by using the 1.4-kb probe and the Genius System (20). The cDNA inserts were characterized by conventional restriction endonuclease mapping procedures. The nucleotide sequence was determined on both strands by the dideoxynucleotide chain-termination method (21) using the Sequenase sequencing kit (United States Biochemical). Nucleotide sequences were analyzed by using the Genetics Computer Group (Madison, WI) programs (22).

Functional Expression in *Xenopus* Oocytes. cRNA was synthesized directly from the human NMDA-receptor subunit 1 (hNR1) clone in the SK(−) vector by *in vitro* transcription with

The publication costs of this article were defrayed in part by page charge payment. This article must therefore be hereby marked "*advertisement*" in accordance with 18 U.S.C. §1734 solely to indicate this fact.

Abbreviations: NMDA, *N*-methyl-D-aspartate; APV, 2-amino-5-phosphovaleric acid; *I*, current; *V*, voltage; hNR1, human NMDA-receptor subunit 1; rNR1, rat NMDA receptor subunit 1; PCP, phencyclidine.

*To whom reprint requests should be addressed.

†The sequence reported in this paper has been deposited in the GenBank data base (accession no. L05666).

T7 polymerase (18). Isolated-follicle free-stage V and VI oocytes of *X. laevis* were injected (50 nl) with cRNA (0.4 mg/ml in diethylpyrocarbonate-treated water) and maintained as described (18, 23). For electrophysiological measurements, oocytes (2–6 days) were transferred to the recording chamber (vol = 0.2 ml) and continuously perfused (2 ml/min) with Ca^{2+}-Ringer solution (115 mM NaCl/2.5 mM KCl/1.8 mM $CaCl_2$/5 mM *N*-tris[hydroxymethyl]-2-aminoethanesulfonic acid (TES) (pH 7.4), in the presence or absence of tested ligands (18). Na^+-free Ringer solution was 115 mM *N*-methylglucamine/3 mM KCl/10 mM $CaCl_2$/5 mM TES, pH 7.4. Ba^{2+}-Ringer solution was identical to Ca^{2+}-Ringer solution but with 1.8 mM $BaCl_2$ instead of $CaCl_2$. Stock solutions (100 mM) of *N*-allylnormetazocine (SKF-10,147), 7-chlorokynurenic acid, and 6-cyano-7-nitroquinoxaline-2,3-dione (CNQX) were prepared in dimethyl sulfoxide. Phencyclidine (PCP) was dissolved in methanol. Dimethyl sulfoxide and methanol in final solutions were <0.01%.

Whole-cell currents were recorded with a conventional two-microelectrode voltage-clamp amplifier (Turbo TEC 01C, NPi Electronics, Tamm, F.R.G.) (18, 23). Only oocytes with resting potentials ≤ -30 mV were studied. All experiments were done at 22 ± 2°C. All processed data are reported as mean ± SD with $n \geq 4$, unless otherwise indicated.

RESULTS AND DISCUSSION

Isolation and Characterization of cDNA Clones. Hybridization screenings yielded several clones. One cDNA clone, denoted as hNR1, is 3.2 kb in length and spanned the entire coding region of the rat rNR1. Analysis of the hNR1 nucleotide sequence revealed the presence of an open reading frame of ≈2.7 kb, coding for a polypeptide of 885 amino acids. Sequence comparison between hNR1 and rNR1 revealed that a 466-bp fragment (from nt 2587 to 3053) from the rat sequence was absent in the human sequence. Different NR1 splice variants derived from the rat brain NR1-encoding gene have been isolated (1, 13–16). hNR1 is a splice variant corresponding to the rodent NR1E species (13). Restriction analysis of other partial cDNA clones isolated from the human library shows that they correspond to other splice variants. These results suggest that, as in rat brain, the NR1 primary transcript undergoes extensive alternative splicing in human brain.

Primary Sequence. Fig. 1 shows an alignment of the deduced amino acid sequences of hNR1, rNR1, and the human brain glutamate receptor 1 of the kainate subtype, denoted as HBGR1 (18). The human brain hNR1 sequence is 97% identical to the rat brain rNR1. The two sequences diverge widely starting at Q846, presumably an exon–intron splice junction. This splice site occurs ≈30 amino acids after the predicted fourth transmembrane segment. The resulting human sequence is 53 amino acids shorter than the rat sequence. Alignment data (25) and hydrophobicity plots (26) disclose the occurrence of several canonical structural features postulated for other members of the superfamily of ligand-gated ion channels (1, 27): there are four potential transmembrane segments, M1–M4 (shown in boxes), that determine a protein topology with a large extracellular N terminus, presumably containing the ligand-binding site. Potential glycosylation sites, indicated by triangles, are confined to the N-terminal segment preceding M1. The long intracellular loop between M3 and M4 contains consensus phosphorylation sites for cAMP-dependent protein kinase (S748), protein kinase C (S658, T665, and S723), calmodulin-dependent protein kinase II (S669, S695, and T730), and tyrosine kinases (Y663 and

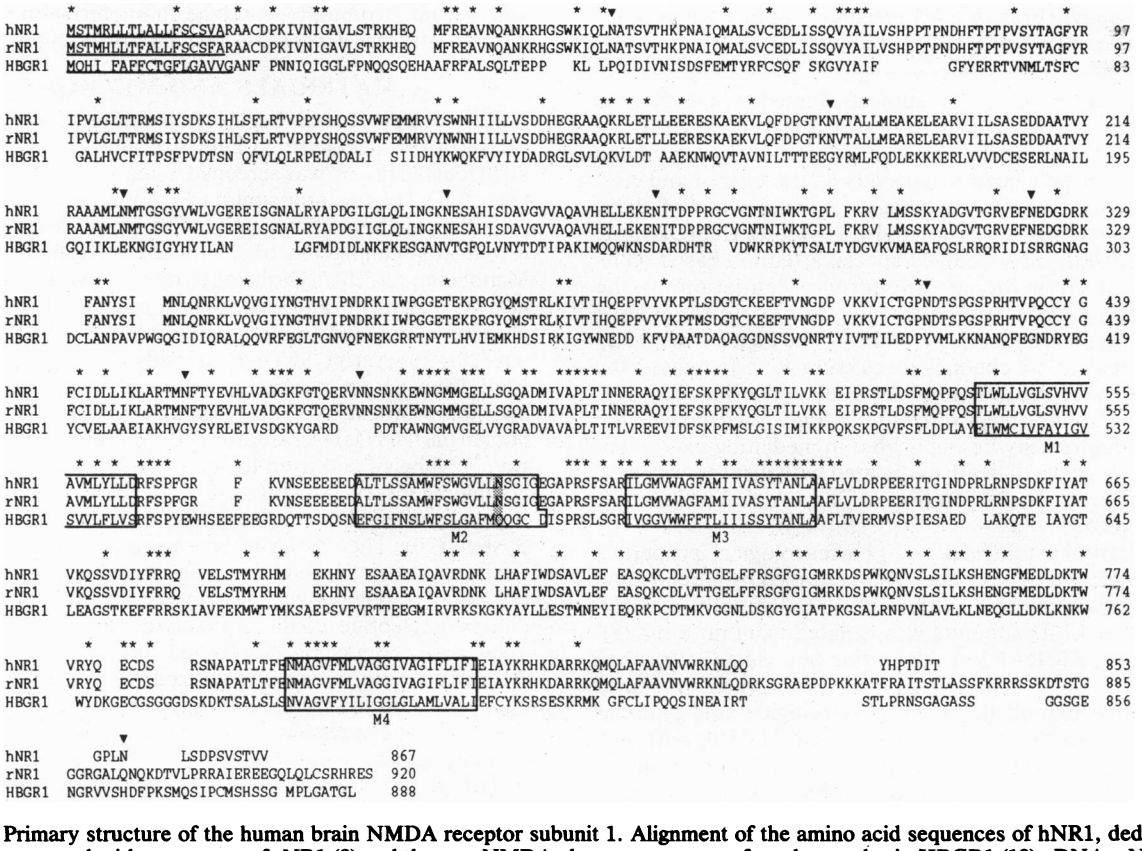

FIG. 1. Primary structure of the human brain NMDA receptor subunit 1. Alignment of the amino acid sequences of hNR1, deduced from its cDNA, compared with sequences of rNR1 (8) and the non-NMDA glutamate receptor from human brain HBGR1 (18) cDNAs. Numbers at right correspond to amino acid positions. Residues are numbered from the first amino acid of the presumed mature protein. Gaps are introduced into the sequences to allow for maximum homology between the three polypeptides. Asterisks (*) denote identical residues in all three proteins; signal peptides are underlined; proposed transmembrane segments M1–M4 are enclosed in boxes. Residues at the Asn-598 position, which determine critical aspects of ion permeability (24), are stippled. Triangles (▼) indicate potential N-glycosylation sites for hNR1. hNR1 differs from rNR1 before Q846 only in residues R14(-), L10(-), V2(-), S141, K194, L249, and L397. Standard one-letter amino acid code is used.

Y693), in accord with the proposed folding of the receptor protein within the cell membrane.

At the amino acid level, sequence identity between either hNR1 or rNR1 and HBGR1 is only 23% (Fig. 1). Sequence similarity and conservation among them are highest in the predicted transmembrane segments and in the region preceding M1. Transmembrane segment M2 of hNR1 and rNR1, considered to form the channel lining, contains an asparagine residue (N598, stippled) that determines the high Ca^{2+} permeability of the receptor channel (24). The long N-terminal extracellular segment that precedes M1 is postulated to contain the agonist-binding site. Site-directed mutagenesis of charged residues in this region of the murine glutamate receptor α_1 subunit has disclosed the occurrence of at least three charged residues critical for L-glutamate binding (28): Glu-398, Asp-443, and Lys-445. Whereas Glu-398 is highly conserved in non-NMDA receptors but is absent in NMDA receptors (Glu-398 in HBGR1), Asp-443 and Lys-445 are identical in HBGR1 (Asp-443 and Lys-445) and in hNR1 or rNR1 (Asp-463 and Lys-465). These conserved residues may contribute to the folding motif that underlies ligand binding in NR1 receptors.

hNR1 Clone Expresses Functional Homomeric Receptor Channels in *X. Laevis* Oocytes. Oocytes injected with cRNA synthesized from the hNR1 clone expressed NMDA-receptor channel activity (Fig. 2*A*). Inward currents were elicited upon perfusion of oocytes with glutamate receptor agonists, according to the pulse protocol displayed under the current traces. Perfusion with 100 μM L-glutamate/10 μM glycine (pulse ON) evoked an inward current that rapidly activates to a peak value and decays to a steady level. The L-glutamate-evoked response was terminated when the agonist was washed out (pulse OFF). NMDA mimics the L-glutamate-activated responses (second and sixth pulse). Quisqualate elicited a signal of much smaller amplitude than those observed with L-glutamate or NMDA (fourth pulse). In contrast, no or negligible responses were observed when the oocyte was exposed to kainate or α-amino-3-hydroxy-5-methyl-4-isoxazole propionic acid (AMPA), specific agonists of non-NMDA receptors (3). Glutamate/NMDA-activated responses were not detected in either noninjected oocytes or oocytes injected with diethylpyrocarbonate-treated water. Based on this assay, the rank of agonist potency at a fixed ligand concentration (100 μM) was L-glutamate > NMDA >> quisqualate >>> AMPA ≈kainate.

Glutamate/NMDA-activated signals strictly depended on the presence of glycine, an allosteric potentiator of NMDA receptors (3) (Fig. 2*B*). In the absence of glycine, L-glutamate failed to elicit detectable inward currents (first pulse). A similar effect was observed with NMDA (data not shown). Agonist-evoked inward currents are recovered by supplementing the agonist solution with μM concentrations of glycine (second pulse). The glycine concentration at which the glutamate-activated currents were 50% of the maximum, determined from best fits to binding isotherms, was 0.45 ± 0.15 μM with a Hill coefficient of 1.5 ± 0.5 (n = 4). Application of 50 μM 7-chlorokynurenic acid, a selective antagonist acting at the glycine modulatory site (3), reduced the current evoked by 100 μM L-glutamate in the presence of a saturating concentration of glycine (10 μM) by 75 ± 4%. Thus, hNR1 receptor channels contain a glycine modulatory site. Consequently, all electrophysiological measurements were done in the presence of glycine.

hNR1 receptor channels expressed in oocytes were blocked by APV and MK-801 {(+)-5-methyl-10,11-dihydro-5*H*-dibenzo[*a*,*d*]cyclohepten-5,10-imine maleate}, specific antagonist and open channel blocker, respectively, of NMDA receptors (3). As displayed in Fig. 2*C*, application of 100 μM NMDA activates an inward current that collapses upon perfusion with 50 μM APV (APV-pulse ON). The NMDA-elicited signal is recovered when APV is removed upon perfusion with NMDA/Ringer solution (APV-pulse OFF). Similarly, addition of 1 μM MK-801 abolished the agonist-induced current (MK-801-pulse ON). MK-801-blocked hNR1 signals were difficult to recover by washing the blocker out, reflecting a very slow dissociation of this open channel blocker from the NMDA receptor channel (29). L-glutamate- and NMDA-evoked signals were blocked at a holding potential V_h = −80 mV by application of 100 μM Zn^{2+} (89 ± 3%) or 100 μM Mg^{2+} (see Fig. 5) to the external bath solution. In contrast, glutamate-activated inward currents were insensitive to 50 μM 6-cyano-7-nitroquinoxaline, an antagonist of non-NMDA receptors (3, 18).

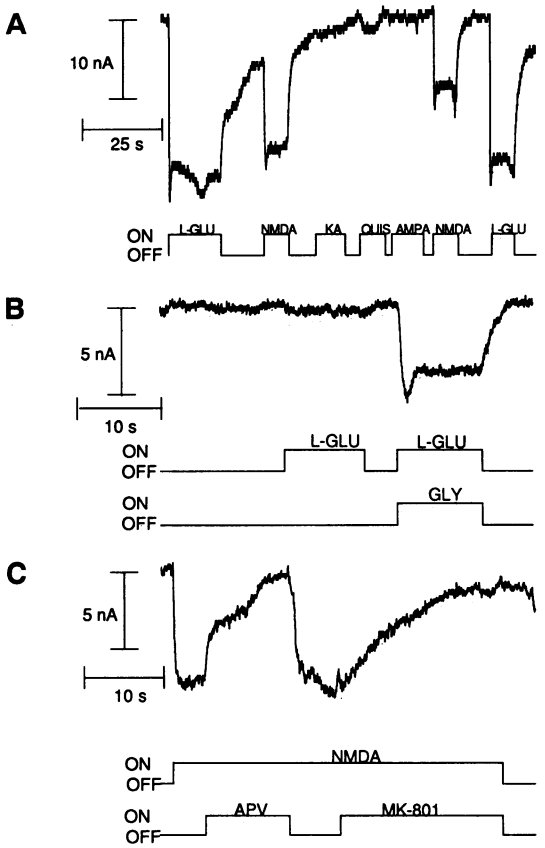

FIG. 2. The hNR1 gene product is an NMDA-selective glutamate receptor. Current responses elicited by glutamate receptor agonists in *X. laevis* oocytes expressing RNA transcripts of hNR1 cDNA. Oocytes were perfused with normal frog Ringer solution supplemented with agonists and/or antagonists as indicated. ON and OFF denote initiation and cessation of perfusion pulse. A downward deflection represents inward current flow. Oocytes were held at −80 mV. Agonist concentration was 100 μM/10 μM glycine except for first pulse in *B*, in which glycine was omitted. 2-Amino-5-phosphovaleric acid (APV) and MK-801 concentrations were 50 μM and 1 μM, respectively. Records were digitized at 100 Hz and filtered at 50 Hz. Current traces are representative of four different oocytes. L-GLU, L-glutamate; GLY, glycine; KA, kainate; Quis, quisqualate; AMPA, α-amino-3-hydroxy-5-methyl-4-isoxazole propionic acid.

PCP, the σ-opioid benzomorphan SKF-10,047, and the dissociative anesthetic ketamine, all of which act on the PCP site (3), are potent blockers of homomeric hNR1 channels. PCP (200 nM), SKF-10,047 (5 μM), and ketamine (10 μM) abrogated the glutamate-activated currents. The inhibitor concentrations at which the current amplitudes were 50% of the maximal response were 100 nM (n = 6) for MK-801, 100 nM (n = 6) for PCP, 0.5 μM for SKF 10,047 (n = 5), and 1 μM (n = 3) for ketamine. Accordingly, the ranking of potency and efficacy is MK-801 ≈PCP > SKF-10,047 > ketamine.

Together, these results indicate that the five sites recognized in NMDA receptors are contained in hNR1 homomeric

receptor channels—namely, the NMDA, glycine, Mg^{2+}, Zn^{2+}, and PCP sites (3, 4, 7). Thus, the ionic currents generated in oocytes expressing the hNR1 gene product display the agonist selectivity and antagonist sensitivity characteristic of the neuronal NMDA receptor (30).

L-Glutamate and NMDA are Potent Agonists of Homomeric hNR1 Receptor Channels. L-glutamate and NMDA displayed the highest potency in activating hNR1 receptor channels (Fig. 2*A*). L-Glutamate-elicited responses were ≈2-fold larger than those evoked by NMDA (Figs. 2*A* and 3*A*). *I* amplitudes were small: 4 nA ≤ *I* ≤ 60 nA, $n = 92$ for 100 μM L-glutamate. Similar observations were reported for the NR1 subunit of rodent and murine brain homologs (8, 9, 14). In contrast, NR2 subunits from rat and mouse brain failed to assemble functional receptors when expressed in oocytes (10–12). Interestingly, heterooligomers obtained by coexpressing NR1A with any of the NR2 subunits cloned thus far exhibit 100-fold larger glutamate-activated currents than those observed by NR1A homooligomers (10, 12).

To assess specificity of the receptor channel encoded by hNR1, dose–response curves for L-glutamate and NMDA were determined (Fig. 3*B*). The agonist concentrations at which the current amplitudes were 50% of the maximal responses (EC_{50}) were 3.7 ± 0.2 μM ($n = 4$) for L-glutamate and 25 ± 9 μM ($n = 3$) for NMDA and were best-fitted with Hill coefficients of 1.7 ± 0.4 and 1.9 ± 0.2. These values are in good agreement with those reported for the rat brain homologs NR1A and NR1B (8, 14). However, the EC_{50} for L-glutamate is 5-fold and 3-fold higher for the hNR1 than for the rat brain gene products NR1A and NR1B (8, 14). Hence, the agonist efficacy of expressed homomeric NMDA receptors appears to depend on the splicing variant.

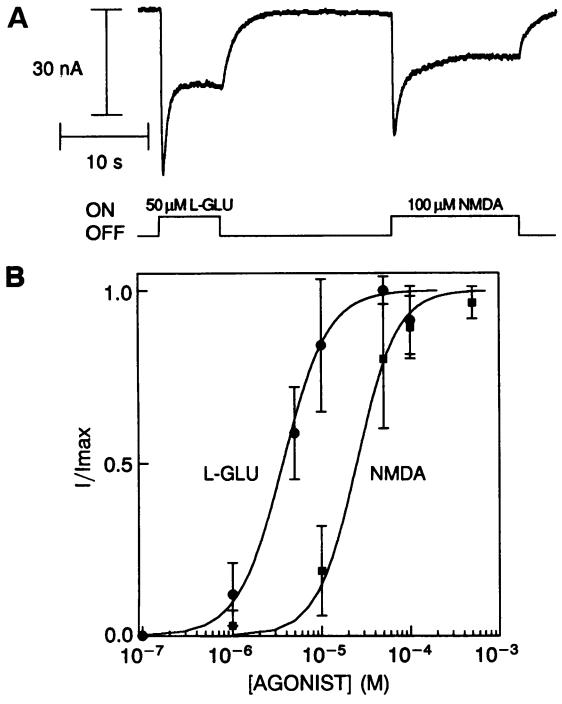

FIG. 3. L-Glutamate and NMDA show high agonist potency and efficacy for hNR1 receptor channels expressed in *X. laevis* oocytes. (*A*) Ionic currents activated by L-glutamate and NMDA in one oocyte expressing the hNR1 gene product. Currents were digitized at 500 Hz and filtered at 300 Hz. (*B*) Dose–response curves. L-Glutamate (●)- and NMDA (■)-activated currents at $V_h = -80$ mV. Agonist solutions were supplemented with 10 μM glycine. Each point represents the mean ± SD, with $n = 4$ for L-glutamate and $n = 3$ for NMDA. Dose–responses for L-glutamate and NMDA were measured in the same oocytes. Solid lines depict theoretical fits to a Michaelis–Menten binding isotherm given by $I/I_{max} = K[\text{agonist}]^n/(1 + K[\text{agonist}]^n)$, where *I* denotes the peak current amplitude at a given agonist concentration, I_{max} is the maximal current estimated from the best fit to the above function, *n* is the number of ligand-binding sites, and *K* is the efficacy constant for the agonist concentration at which response is half-maximal ($I_{max}/2$). Other conditions as described in the legend for Fig. 2.

hNR1 Receptor Channels are Permeable to Calcium Ions. L-Glutamate and NMDA-elicited responses are biphasic, exhibiting a transient current that rapidly decays to a steady level (Fig. 3*A*). The peak current has been associated with the activation of an endogenous Ca^{2+}-dependent chloride channel (31) resulting from calcium influx through NMDA receptors (32). The current amplitude depends on the extracellular calcium concentration (Fig. 4): a 10-fold increase of calcium concentration augmented both the peak and the plateau currents. In contrast, bathing the oocyte in Ba^{2+}-Ringer solution (in the absence of Ca^{2+}) prevents occurrence of the transient component, slightly reduces amplitude of the steady-level current (Fig. 4), and shifts reversal potential toward more positive values (data not shown). The chloride channel blockers, flufenamic (100 μM) and niflumic acid (100 μM) (32), attenuated the transient component of the L-glutamate-evoked inward currents in Ca^{2+}-Ringer solution (data not shown) and, as in Ba^{2+}-Ringer solution, the current reversed at positive potentials (Fig. 5*C*). Taken together, these results suggest that the fast desensitizing component of the L-glutamate-activated currents is accounted for, at least in part, by the activation of endogenous calcium-dependent chloride channels consequent to Ca^{2+} influx through hNR1 receptor channels and, therefore, indicate that homomeric hNR1 receptor channels are permeable to Ca^{2+}, as are the natural NMDA-sensitive receptors in neurons (3, 7).

Homomeric hNR1 Receptor Channels are Blocked by Mg^{2+} in a Voltage-Dependent Manner. A specific feature of NMDA receptors is their voltage-dependent sensitivity to extracellular Mg^{2+} blockade (6). As displayed in Fig. 5*A*, at a holding potential of −80 mV, perfusion of oocytes with 100 μM L-glutamate evokes an inward current. Application of 100 μM $MgCl_2$ (Mg^{2+}-pulse ON) attenuates the L-glutamate-elicited response and prevents further current generation as long as it remains in the external bathing medium. L-Glutamate-activated currents are restored as the magnesium is washed out (Mg^{2+}-pulse OFF). In contrast, when the oocyte is held at −40 mV the blocking effect exerted by extracellular Mg^{2+} is less effective (Fig. 5*B*).

To rigorously assess the voltage dependence of hNR1 receptor channel blockade by Mg^{2+}, the *I–V* relationship was studied (Fig. 5*C*) using a ramp protocol (10). In the absence of Mg^{2+}, hNR1 channels display a linear *I–V* relationship

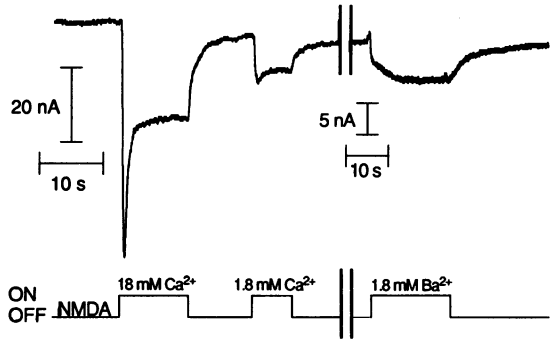

FIG. 4. hNR1 homooligomer receptor channels are calcium permeable. Current responses activated by NMDA at −80 mV upon perfusion of oocytes with different Ringer solutions. Eighteen millimolar Ca^{2+} denotes high Ca^{2+}-Ringer (95 mM NaCl/18 mM $CaCl_2$/2.8 mM KCl/5 mM TES, pH 7.4), 1.8 mM Ca^{2+} is normal frog Ringer solution, and 1.8 mM Ba^{2+} refers to Ba^{2+}-Ringer solution. Vertical bars denote a different oocyte. Other conditions are as described in the legend for Fig. 2.

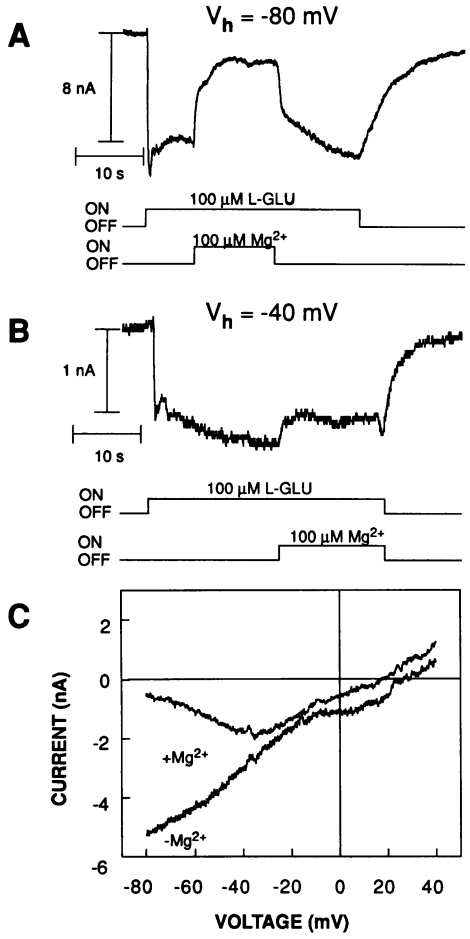

FIG. 5. Voltage-dependent blockade of hNR1 receptor channels by Mg^{2+}. (*A* and *B*) L-Glutamate (L-GLU)-activated ionic currents at −80 mV and −40 mV. Oocytes were perfused with L-glutamate alone or supplemented with $MgCl_2$, as indicated. (*C*) *I–V* relation of L-glutamate-activated responses (100 μM) in the absence (−Mg^{2+}) or presence (+Mg^{2+}) of 100 μM $MgCl_2$. L-Glutamate and frog Ringer solutions were supplemented with 100 μM flufenamic acid and 100 μM niflumic acid. Oocytes were held at −80 mV, perfused with agonist, and depolarized to 40 mV in 2 s (60 mV/s) using a ramp protocol (PCLAMP 5.5). Leak currents were determined in the absence of agonist and subtracted from the glutamate-activated currents. Each trace consists of 2000 points and represents the average of at least three oocytes. Other conditions were as described in the legend for Fig. 2.

with a reversal potential of ≈+20 mV (in the presence of chloride channel blockers). In the presence of Mg^{2+}, the L-glutamate-evoked currents exhibit a conspicuous rectification (Fig. 5*C*): Mg^{2+}-induced blockade occurs only at negative potentials and decreases with membrane depolarization. As a result, the linear *I–V* relationship obtained in the absence of Mg^{2+} is transformed to a nonlinear function in its presence, features displayed by the NMDA receptor in the central nervous system (6).

hNR1 Codes for a Glutamate-Sensitive Receptor of the NMDA Subtype. The results show that the gene product encoded by the hNR1 cDNA clone expressed in amphibian oocytes reproduces the complex functional and pharmacological features characteristic of NMDA-receptor channel in neurons. Therefore, hNR1 codes for a human brain NMDA receptor subunit. Availability of cDNA clones for human brain NMDA receptors and their expression in heterologous systems thus provide a powerful system for a detailed investigation of the pharmacological properties of human brain receptors and, in combination with molecular modeling of the pore-forming structure, may provide insights toward the development of site-directed drug design.

R.P.-C. and W.S. are both considered first authors and are listed alphabetically. We thank S. Nakanishi for the NMDAR1A clone, M. Geyer for ketamine, J. Tomich and B. Cai for oligonucleotides, S. Lee for RNA preparation, D. Hoang for sequencing, and R. Blewitt for sequence analysis. This work was supported by a grant from the National Institutes of Health (MH-44638) and by a Research Scientist Award from the Alcohol, Drug Abuse and Mental Health Administration (MH-00778) to M.M. W.S. is a Predoctoral Trainee (NIH 5T32GM08326). A.V.F.-M. is a Postdoctoral Fellow of the North Atlantic Treaty Organization.

1. Nakanishi, S. (1992) *Science* **258,** 597–603.
2. Choi, D. (1992) *Science* **258,** 241–243.
3. Collingridge, G. L. & Lester, R. A. J. (1989) *Pharmacol. Rev.* **40,** 143–210.
4. Madison, D. V., Malenka, R. C. & Nicoll, R. A. (1991) *Annu. Rev. Neurosci.* **14,** 379–397.
5. Choi, D. W. & Rothman, S. M. (1990) *Annu. Rev. Neurosci.* **13,** 171–182.
6. Ascher, P. & Nowak, L. (1988) *J. Physiol. (London)* **399,** 247–266.
7. Mayer, M. L. & Westbrook, G. L. (1987) *J. Physiol. (London)* **394,** 501–527.
8. Moriyoshi, K., Masu, M., Takahiro, I., Shigemoto, R., Mizuno, N. & Nakanishi, S. (1991) *Nature (London)* **354,** 31–37.
9. Yamazaki, M., Mori, H., Araki, D., Mori, K. J. & Mishina, M. (1992) *FEBS Lett.* **300,** 39–45.
10. Monyer, H., Sprengel, R., Schoepfer, R., Herb, A., Higuchi, M., Lomeli, H., Burnashev, N., Sakmann, B. & Seeburg, P. (1992) *Science* **256,** 1217–1221.
11. Kutsuwada, T., Kashiwabuchi, N., Mori, H., Sakimura, K., Kushiya, E., Araki, K., Meguro, H., Masaki, H., Kumanishi, T., Arakawa, M. & Mishina, M. (1992) *Nature (London)* **358,** 36–41.
12. Meguro, H., Mori, H., Araki, K., Kushiya, E., Kutsuwada, R., Yamazaki, M., Kumanishi, T., Arakawa, M., Sakimura, K. & Mishina, M. (1992) *Nature (London)* **357,** 70–74.
13. Sugihara, H., Moriyoshi, K., Ishii, T., Masu, M. & Nakanishi, S. (1992) *Biochem. Biophys. Res. Commun.* **185,** 826–832.
14. Nakanishi, N., Axel, R., & Shneider, N. A. (1992) *Proc. Natl. Acad. Sci. USA* **89,** 8552–8556.
15. Durand, G. M., Gregor, P., Zheng, X., Bennett, M. V. L., Uhl, G. R. & Zukin, R. S. (1992) *Proc. Natl. Acad. Sci. USA* **89,** 9359–9363.
16. Anantharam, V., Panchal, R. G., Wilson, A., Kolchine, V. V., Treitsman, S. N. & Bayley, H. (1992) *FEBS Lett.* **305,** 27–30.
17. Weller, M. & Kornhuber, J. (1992) *Arch. Neurol.* **49,** 900–901.
18. Sun, W., Ferrer-Montiel, A. V., Schinder, A. F., McPherson, J. P., Evans, G. A. & Montal, M. (1992) *Proc. Natl. Acad. Sci. USA* **89,** 1443–1447.
19. Ahmed, C. M. I., Ware, D. H., Lee, S. C., Patten, C. D., Ferrer-Montiel, A. V., Schinder, A. F., McPherson, J. P., Wagner-McPherson, K., Wasmuth, J. J., Evans, G. A. & Montal, M. (1992) *Proc. Natl. Acad. Sci. USA* **89,** 8220–8224.
20. Martin, R., Hoover, C., Grimme, S., Crogan, C., Holtke, J. & Kessler, C. (1990) *BioTechniques* **9,** 762–768.
21. Sanger, F., Nicklen, S. & Coulson, A. R. (1977) *Proc. Natl. Acad. Sci. USA* **74,** 5463–5467.
22. Devereux, J., Haeberli, P. & Smithies, O. (1984) *Nucleic Acids Res.* **12,** 387–395.
23. Methfessel, C., Witzemann, V., Takahasni, T., Mishina, M., Numa, S. & Sakmann, B. (1986) *Pflügers Arch.* **407,** 577–588.
24. Burnashev, N., Schoepfer, R., Monyer, H., Ruppersberg, J. P., Günther, W., Seeburg, P. H. & Sakmann, B. (1992) *Science* **257,** 1415–1419.
25. Feng, D. F. & Doolittle, R. G. (1990) *Methods Enzymol.* **183,** 375–387.
26. Klein, P., Kanehisa, M. & DeLisi, C. (1985) *Biochim. Biophys. Acta* **815,** 468–476.
27. Numa, S. (1989) *Harvey Lect.* **83,** 121–165.
28. Uchino, S., Sakimura, K., Nagahari, K. & Mishina, M. (1992) *FEBS Lett.* **308,** 253–257.
29. Wong, E. H. F., Kemp, J. A., Priestley, T., Knight, A. R., Woodruff, G. N. & Iversen, L. L. (1986) *Proc. Natl. Acad. Sci. USA* **83,** 7104–7108.
30. Patneau, D. K. & Mayer, M. L. (1990) *J. Neurosci.* **10,** 2385–2399.
31. Miledi, R. & Parker, I. (1984) *J. Physiol. (London)* **357,** 173–183.
32. Leonard, J. P. & Kelso, S. R. (1990) *Neuron* **4,** 53–60.